High-Power and High-Speed Zn-Diffusion Single Fundamental-Mode Vertical-Cavity Surface-Emitting Lasers at 850-nm Wavelength

J.-W. Shi, C.-C. Chen, Y.-S. Wu, S.-H. Guol, Chihping Kuo, and Ying-Jay Yang

***Abstract*—We demonstrate a high-performance Zn-diffusion single-mode 850-nm vertical-cavity surface-emitting laser, which has a low threshold current (0.5 mA), high differential efficiency (80%), high modulation current efficiency (8.2 GHz/mA$^{1/2}$), and can sustain the single fundamental-mode output with a maximum output power of 7.3 mW under the full range of bias currents. With this device we can achieve 10 Gb/s eye-opening at a low bias current (1.8 mA) and a peak-to-peak driving-voltage of 0.5 V, which corresponds to a very high data-rate/power-dissipation ratio of 6.5 Gps/mW.**

***Index Terms*—Semiconductor laser, vertical-cavity surface-emitting laser (VCSEL).**

I. Introduction

HIGH-POWER and single-mode vertical-cavity surface-emitting lasers (VCSELs) that operate at a wavelength of 850 nm have lately attracted a lot of attention and can be used for a variety of applications: e.g., in laser printing [1], [2] and to enhance the resolution of airborne light detecting and ranging (LIDAR) systems [1], [3]. The use of this type of single-mode VCSEL is also becoming increasingly important in the area of short-reach fiber communication and optical inter- or intra-board computer bus systems [4]. The application of a VCSEL array, which has single-mode performance for each VCSEL unit, to a high-speed parallel optical interconnect, allows one to take advantage of the small far-field divergence angle $(\sim 8^{\circ})$ of the single-mode VCSEL, thereby avoiding serious optical crosstalk between neighboring emitters, as well as bringing the additional benefit of the downscaling of the spacing between single elements in the array. These issues can be expected to become more and more important as the bus-line density continues to increase with the total bandwidth capacity of the system. Several methods, such as surface relief structures [4], [5], triangular holey structures [6], and anti-resonant reflecting optical waveguide structures [7], have been utilized to fabricate VCSELs with a relatively large active diameter, a single-mode, and high output optical power performance. A triangular holey structure [6] with a 5-mA threshold current has demonstrated a state-of-the-art single-mode power of 7.5 mW with stable polarization output. Again, a surface relief VCSEL has been developed which demonstrates excellent dynamic performance with a low threshold current (0.5 mA) and high single-mode output power (4.6 mW) [5]. In this letter, we demonstrate the state-of-the-art performance of a Zn-diffusion single-mode 850-nm VCSEL [8], i.e., high single-mode output power (7.3 mW) and low threshold current (0.5 mA). The high external efficiency (around 80%) and low threshold current of our device makes it possible to achieve clear eye-opening of 10 Gb/s at a bias current of 1.8 mA and a peak-to-peak driving-voltage of 0.5 V, which corresponds to a very high data-rate/power-dissipation ratio of 6.5 Gps/mW [9].

Manuscript received December 26, 2007; revised March 10, 2008. This work was supported by the National Science Council of Taiwan under Grant NSC-96-2221-E-008-121-MY3.

J.-W. Shi, C.-C. Chen, and Y.-S. Wu are with the Department of Electrical Engineering, National Central University, Taoyuan 320, Taiwan, R.O.C. (e-mail: jwshi@ee.ncu.edu.tw).

S.-H. Guol is with the Graduate Institute of Electro-Optical Engineering, National Taiwan University, Taipei 106, Taiwan, R.O.C.

C. Kuo is with Luxnet Corporation, Taoyuan 325, Taiwan, R.O.C.

Y.-J. Yang is with the Department of Electrical Engineering, National Taiwan University, Taipei 106, Taiwan, R.O.C.

Color versions of some of the figures in this letter are available online at http://ieeexplore.ieee.org.

Digital Object Identifier 10.1109/LPT.2008.924645

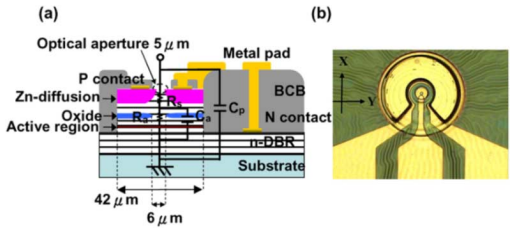

Fig. 1. (a) Cross-sectional view and (b) top-view of our device. The x and y axes, which are specified in our far-field measurement, are defined in (b).

II. Device Structure and Fabrication

Fig. 1(a) and (b) shows the conceptual cross-sectional and top views of the demonstrated device. An equivalent-circuit-model, which is used for device modeling, is also illustrated in Fig. 1(a) [8]. The epilayer structure, purchased from IQE (IEGENS-7-20), is composed of three GaAs–$Al_{0.3}Ga_{0.7}As$ multiple-quantum-wells (MQWs) sandwiched between a 30-pair n-type and 20-pair p-type $Al_{0.9}Ga_{0.1}As$–$Al_{0.12}Ga_{0.88}As$ distributed-Bragg-reflector (DBR) layers with an $Al_{0.98}Ga_{0.02}As$ layer (30-nm thickness) just above the MQWs for oxidation. An oxidation technique is used to define a circular current-confined area 6 μm in diameter, which is much larger than the less than 3-μm diameter of the 850-nm single-mode oxide-confined VCSELs [4]. The diameter of the optical aperture (without Zn-diffusion) is around 5 μm to ensure single-mode operation, as shown in Fig. 1(a) [8]. Lasing is suppressed in the Zn-diffused DBR region due to free-carrier absorption and reflectivity reduction caused by disordering [8]. As can be seen by a comparison with our previous work [8], we were able to downscale the diameter

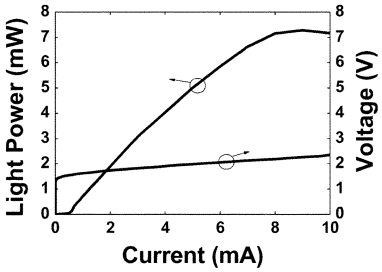

Fig. 2. Characteristics of the optical output power (L) and voltage (V) versus biasing current (I) of our device.

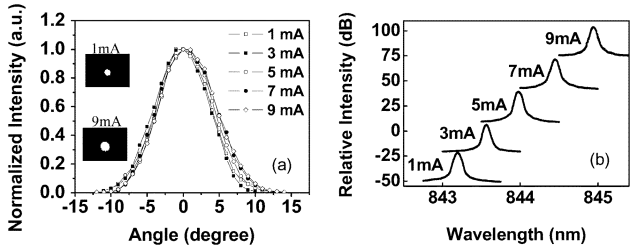

Fig. 3. (a) Measured 1-D far-field patterns in the x directions under different current levels. The insets show 2-D images of the far-field patterns under low (near threshold) and high bias currents (near saturation). (b) The measured output optical spectra under different bias currents.

of the oxide-confined aperture from 9 to 6 μm, which allows us to reduce the threshold current and minimize the misalignment between the Zn-diffusion aperture and the oxide-confined aperture, which greatly improves the performance of the device. Details of the fabrication process have been given in our previous work [8].

III. Measurement Results

Fig. 2 shows the light output versus current (L–I) and the bias current versus voltage (I–V) characteristics of our device. The measured L–I curve clearly shows a threshold current and maximum output power of around 0.5 mA and 7.3 mW, respectively, with a maximum external quantum efficiency of as high as 80%. The measured I–V curves indicate that the device has a differential resistance of around 78 Ω, which is much lower than that typically reported for high-speed single-mode VCSELs ($\sim$200 Ω [4]). This was possible because of the larger active diameter and the deposition of the p-type ohmic contacts on the Zn-diffused region, which led to disordering of the DBR layers and reduced device resistance [8]. The 1-D far-field patterns of our device were measured under different operating currents using a rotational arm, a mounted slit, and a photodetector. The results are shown in Fig. 3(a). The insets to (a) show 2-D images of the far-field patterns obtained under low bias currents (near the threshold) and high bias currents (near saturation). We can clearly see that single-spot device output can be achieved for the whole range of bias currents (from near the threshold to saturation). Furthermore, the measured full-width at half-maximum (FWHM) of the far-field pattern is around 9°, which is close to the calculated ideal diffraction-limited divergence angle (around 8°) of a Zn-diffusion aperture with a diameter of less than 5 μm. Such a result is an indication of the single-fundamental-mode performance of our device [6]. The polarization of the output far field was also measured and shows the problem of instability. This is

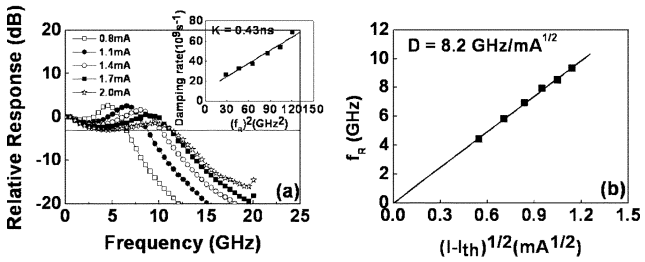

Fig. 4. (a) Measured E-O frequency responses under different bias currents. The inset shows the extracted K-factors. (b) The measured relaxation oscillation frequency versus $(I - I_{\rm th})^{1/2}$ and the extracted D factor.

similar to the phenomenon reported for a single-mode surface relief 850-nm VCSEL and may be attributed to an increase of junction temperature-induced polarization change [10]. Such polarization instability-induced noise can be overcome by further modifying the geometric structure of our Zn-diffusion VCSEL to stabilize the polarization of output [11]. Fig. 3(b) shows the output optical spectra measured during high-speed measurement. During this process our device was modulated by a radio-frequency (RF) signal with a power of around -7 dBm. The collected optical signal was sent to a high-speed photoreceiver with a 3-dB bandwidth of 12 GHz (New focus 1580-B) or an optical spectrum analyzer (ANDO AQ6315A), to record the electrooptic (E-O) frequency response and optical spectra, respectively. We can clearly see that even under the highest saturation bias current (9 mA), the device could still maintain single-mode operation, with a side-mode suppression ratio (SMSR) of all the traces of over 25 dB. The measurement results shown in Figs. 2 and 3 show that our device can sustain single-fundamental-mode operation under the whole range of bias currents with an extremely high maximum single-mode power (7.3 mW). The high-speed E-O performance of the fabricated devices was measured by a lightwave component analyzer (LCA), which was composed of a network analyzer (Anritsu 37397C) and a calibrated photoreceiver module (New focus 1580-B).

The measured frequency responses of the microwave reflection (S_{11}) and the equivalent-circuit-model fitting show that the RC-limited bandwidth of the device is around 15 GHz. Fig. 4(a) shows the measured E-O frequency responses under different bias currents. The inset to (a) shows the square of the relaxation oscillation (RO) frequency (f_R) versus damping rate (γ) that were derived by fitting the E-O modulation responses in this figure through the use of extracted RC-limited frequency responses of our device and the formulas reported in [12] and [13]. We can extract the K-factors from the slope of the fitting lines [12], [13] to determine the intrinsic maximum 3-dB bandwidth. The extracted value of the K-factor (0.43 ns), which corresponds to an intrinsic bandwidth of around 20.7 GHz, is close to that reported for a multimode 850-nm VCSEL (0.4 ns) with the same diameter of oxide-confined aperture (6 μm) [13] and is larger than that found for a Zn-diffusion single-mode 850-nm VCSEL discussed in our previous work [8]. This was due to the fact that the newly demonstrated device has a smaller oxide-confined aperture (6 μm versus 9 μm), much higher single-mode output power (7.3 versus 3 mW) and higher photon density [12], [13]. It can be seen by looking at the figures that we can achieve a 3-dB E-O 10-GHz bandwidth under a very low bias current

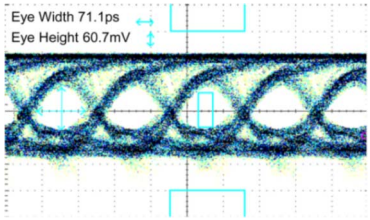

Fig. 5. Measured output eye-diagram with the device connected to a photoreceiver module (New focus 1580-B). The output eye-pattern can pass the OC-192 (10 Gb/s) eye mask.

(1.4 mA). The following can be used to evaluate how fast the relaxation oscillation frequency (3-dB bandwidth) increases with the bias current [13]:

$$f_R = D\sqrt{I - I_{\rm th}} \tag{1}$$

where I is the bias current, and $I_{\rm th}$ is the threshold current. Therefore, a larger D factor indicates that we can use a lower bias current to attain the desired high-speed performance, which is a key issue for optical interconnect applications. Fig. 4(b) shows the f_R as a function of $(I - I_{\rm th})^{1/2}$, and the extracted D factor (8.2 GHz/mA$^{1/2}$). Compared with the values reported for high-speed multimode oxide-confined 850-nm VCSELs [13], [14] with a similar oxide-confined aperture ($\sim$6 μm), those of our demonstrated device have a much larger D factor (8.2 GHz/mA$^{1/2}$ versus $\sim$5 GHz/mA$^{1/2}$). This superior D-factor performance may be attributed to the fact that in the reported multimode VCSELs [13], [14], the spreading of photons among multiple mutually incoherent modes significantly impedes the increase in bandwidth with the photon density (bias current) [15]. Overall, the results imply that our device can achieve a comparable high-speed performance ($\sim$10 GHz) with much lower dc power consumption than that of multimode VCSELs [13], [14]. On the other hand, when the bias current reaches 2 mA, there is a significant low-frequency rolloff and damping which limit the measured 3-dB E-O bandwidth. This phenomenon can be attributed to the spatial hole burning (SHB) effect [12], which is usually observed in single-mode high-power VCSELs and results in serious damping and low-frequency rolloff [12]. Fig. 5 shows the measured noninverted eye-pattern under low power operation (1.8-mA bias current) and the OC-192 eye mask. The same photoreceiver module as in the LCA measurements is used. The input digital signal has a pseudorandom bit sequence of $2^{15}-1$, and a 0.5-V peak-to-peak voltage. We can clearly see that due to its high-efficiency and low-threshold performance, we can achieve clear eye-opening of 10 Gb/s with this device, with extremely small dc power consumption (3.4 mW). We can define the dissipated power of our device as the difference between the output optical output power ($\sim$1.9 mW) and the injected electrical power (3.4 mW). The corresponding data-rate/power-dissipation ratio can be as high as 6.5 Gps/mW, which is comparable to that of a high-performance 980-nm VCSEL suitable for application in optical interconnects (6.5 versus 3.5 Gps/mW) [9].

IV. Conclusion

In this letter, we demonstrate the state-of-the-art performance of a Zn-diffusion 850-nm single- mode VCSEL which includes: high single-mode power (7.3 mW), large D factor (8.2 GHz/mA$^{1/2}$), and low threshold current (0.5 mA). With the device we can achieve 10 Gb/s operation with a high data-rate/power-dissipation ratio (6.5 Gps/mW).

References

[1] R. Szweda, "VCSELs resurgent," *III-Vs Rev. Advanced Semiconductor Mag.*, vol. 17, no. 8, pp. 2–5, Nov. 2004.

[2] H. Otoma, A. Murakami, Y. Kuwata, N. Ueki, N. Mukoyama, T. Kondo, A. Sakamoto, S. Omori, H. Nakayama, and T. Nakamura, "Single-mode oxide-confined VCSEL for printers and sensors," in *Proc. Electronics System Integration Technology Conf.*, Sep. 2006, vol. 1, pp. 80–85.

[3] E. M. Strzelecki, D. A. Cohen, and L. A. Coldren, "Investigation of tunable single frequency diode lasers for sensor applications," *J. Lightw. Technol.*, vol. 6, no. 10, pp. 1610–1618, Oct. 1988.

[4] F. Mederer, I. Ecker, J. Joos, M. Kicherer, H. J. Unold, K. J. Ebeling, M. Grabherr, R. Jäger, R. King, and D. Wiedenmann, "High performance selectively oxidized VCSELs and arrays for parallel high-speed optical interconnects," *IEEE Trans. Adv. Packag.*, vol. 24, no. 4, pp. 442–449, Nov. 2001.

[5] Å. Haglund, J. S. Gustavsson, P. Modh, and A. Larsson, "Dynamic mode stability analysis of surface relief VCSELs under strong RF modulation," *IEEE Photon. Technol. Lett.*, vol. 17, no. 8, pp. 1602–1604, Aug. 2005.

[6] A. Furukawa, S. Sasaki, M. Hoshi, A. Matsuzono, K. Moritoh, and T. Baba, "High-power single-mode vertical-cavity surface-emitting lasers with triangular holey structure," *Appl. Phys. Lett.*, vol. 85, pp. 5161–5163, Nov. 2004.

[7] D. Zhou and L. J. Mawst, "High-power single-mode antiresonant reflecting optical waveguide-type vertical-cavity surface-emitting lasers," *IEEE J. Quantum Electron.*, vol. 38, no. 12, pp. 1599–1606, Dec. 2002.

[8] J.-W. Shi, L.-C. Yang, C.-C. Chen, Y.-S. Wu, S.-H. Guol, and Y.-J. Yang, "Minimization of damping in the electrooptic frequency response of high-speed Zn-diffusion single-mode vertical-cavity surface-emitting lasers," *IEEE Photon. Technol. Lett.*, vol. 19, no. 24, pp. 2057–2059, Dec. 15, 2007.

[9] Y.-C. Chang, C. S. Wang, and L. A. Coldren, "High-efficiency, high-speed VCSELs with 35 Gbit/s error-free operation," *Electron. Lett.*, vol. 43, no. 19, pp. 1022–1023, Sep. 13, 2007.

[10] Å. Haglund, S. J. Gustavsson, J. Vukŭsić, P. Jedrasik, and A. Larsson, "High-power fundamental-mode and polarisation stabilised VCSELs using sub-wavelength surface grating," *Electron. Lett.*, vol. 41, no. 14, pp. 805–807, Jul. 7, 2005.

[11] C. C. Chen, "Vertical-cavity surface-emitting laser with stable single transverse mode and stable polarization," Ph.D. dissertation, National Taiwan University, Taiwan, R.O.C., 2002.

[12] J. S. Gustavsson, A. Haglund, J. Bengtsson, P. Modh, and A. Larsson, "Dynamic behavior of fundamental-mode stabilized VCSELs using shallow surface relief," *IEEE J. Quantum Electron.*, vol. 40, no. 6, pp. 607–619, Jun. 2004.

[13] C. Carlsson, H. Martinsson, R. Schatz, J. Halonen, and A. Larsson, "Analog modulation properties of oxide confined VCSELs at microwave frequencies," *J. Lightw. Technol.*, vol. 20, no. 9, pp. 1740–1749, Sep. 2002.

[14] T. Tanigawa, T. Onishi, S. Nagai, and T. Ueda, "High-speed 850 nm AlGaAs/GaAs vertical cavity surface emitting laser with low parasitic capacitance fabricated using BCB planarization technique," in *Proc. Conf. Lasers Electro-Opt. (CLEO 2005)*, pp. 1381–1383, Paper CWI3.

[15] K. L. Lear and A. N. Al-Omari, "Progress and issues for high speed vertical cavity surface emitting lasers," *Proc. SPIE*, vol. 6484, pp. 64840J-1–64840J-12, 2007.